Analysis and optimization of drilling parameters for tool wear and hole dimensional accuracy in B₄C reinforced Al-alloy

A. TASKESEN[1], K. KUTUKDE[2]

1. Manufacturing Engineering, Gazi University, 06500 Teknikokullar, Ankara, Turkey;
2. Institute of Science and Technology, Gazi University, 06500 Teknikokullar, Ankara, Turkey

Abstract: Cutting parameters were evaluated and optimized based on multiple performance characteristics including tool wear and size error of drilled hole. Taguchi's L_{27}, 3-level, 4-factor orthogonal array was used for the tests. It is shown that generally abrasive wear and built up edge (BUE) formation were seen in the tool wear, and the corner wear was also of major importance. Flank wear of the cutting tool was found to be mostly dependent upon particle mass fraction, followed by feed rate, drill hardness and spindle speed, respectively. Among the tools used, TiAlN coated carbide drills showed the best performance with regard to the tool wear as well as hole size. Grey relational analysis indicated that drill material was the more influential parameter than feed rate and spindle speed. The results revealed that optimal combination of the drilling parameters could be used to obtain both minimum tool wear and diametral error.

Key words: powder metallurgy; B₄C; drilling; tool wear; hole dimensional accuracy; optimization

1 Introduction

Due to their high specific strength, superior wear resistance, lower thermal expansion and lightweight, metal matrix composites (MMCs) are used as substitute for conventional materials in some engineering applications such as aerospace, electronics, automotive, medical and military industries [1−10]. They are preferred in wide variety of applications such as bearings, pistons, connecting rods, automobile brake rotors, sliding electrical contacts, turbo charger impellers, space structures [11,12]. Matrix, reinforcement and nature of the interface affect the properties of these composites, and reinforcement materials are generally used in the form of particles, whiskers or fibers in different fractions ranging from few percentage up to 60% [13]. Selecting and combining of suitable reinforcement and matrix qualification are key factors in their fabrication. Various matrix materials such as Al, Ti and Mg are used, while mostly used reinforcements are SiC, Al₂O₃ and B₄C. In addition, several production methods such as powder metallurgy (PM) and stir casting are used to produce MMCs. The major disadvantages of the latter method are agglomeration of the ceramic reinforcements, formation of porous structure and poor wetting between the particles and matrices [14,15]. On the other hand, PM has some important advantages such as simplicity, cheap processing, homogenous distribution of the reinforcement particles and high quality mechanical properties [16]. However, the machinability of these composites is difficult because of hard abrasive reinforcement particles causing rapid tool wear, thus leading to labor losses, high tool cost, size error, poor surface roughness and less tool life. Therefore, the cutting tool may be used more effectively by knowing the wear mechanisms dependent on the cutting parameters and machining conditions.

2 Literature review

The tool geometry of a drill is more complicated than other cutting tools. Because of this complexity, majority of the researches on the tool wear in drilling are based on the investigation of experimental data [17]. The common wear types in drilling are, in general, crater and flank wear. Owing to the high tool-chip interface temperature, crater wear caused mostly by diffusion occurs on the rake surface where chip flows through the cutting tool. However, flank wear (V_B) is usually

considered as criterion of tool life or a significant guide to assess the tool performance in machining. More than that, two abrasive wear mechanisms namely two-body and three-body are dominant when machining MMCs [18].

Currently, although there are a number of studies on MMCs drilling, limited studies exist on the drilling of B_4C reinforced composites regarding the cutting tool performance and drilled hole size accuracy. Until now, mostly Al_2O_3 and SiC particles, whose hardnesses were HV 2100−2300 (Vickers Hardness) and HV 2700−3500, respectively, were used as reinforcement elements [4,10]. Past studies on the drilling of MMCs stated that the main wear type is flank wear, and abrasive and adhesive wear mechanisms are prevalent in the cutting tool [1−10, 19−21]. Abrasive hard particles create micro grooves on the tool's cutting edge and these grooves get larger with increasing cutting speeds, resulting in built-up edge (BUE) formation by filling these micro grooves with the squeezed workpiece material [10]. Additionally, there has been an increase on BUE formation as the hole number increases [7].

Some earlier researchers argued that the BUE layer plays an important role in the protection of tool-chip surface [9,10]. Nevertheless, other researchers claimed that the continuous slipping of the BUE particles through the tool-chip interface might caus the tool wear [20,22]. From the point of view of cooling, through-tool cooling improves the tool wear and reduces the BUE formation in comparison with the conventional cooling and dry cutting [19,20].

Cutting tool performance is influenced by certain machining parameters such as particle fraction, cutting speed, feed rate and cutting tool material when drilling MMCs. One of the important factors affecting the tool wear is workpiece material, i.e. particle fraction and the matrix. Grinding effect and abrasive forces on the cutting tool, which cause the wear rate to grow, increase as the particle fraction increases [4]. Heat treatment conditions also have an important effect on the tool wear, and the highest tool wear is observed when drilling 18% SiC/Al2618 composite material aged for 20 h [19]. These literature results showed that an increase in the particle fraction or workpiece hardness results in an increase in the tool wear. Nevertheless, due to lubricating property, the inclusion of Ni coated graphite particles to the Al composite causes the tool wear rate to decrease [4].

A study on the drilling of Al356/20/SiC MMCs [8] claimed that the highest influence on the tool wear is cutting time (50%) and the next one is feed rate (24%). It can also be understood from most of the previous studies that tool wear improves with increasing the feed rate due to less contact time between the cutting tool and workpiece [2,3,6,7,10,21]. Moreover, tool wear increases

linearly until the cutting depth of 10 mm and then increases slowly [3].

The next important factor affecting the tool wear is cutting tool material. In the literature, several drill materials such as HSS, carbide and PCD are used when drilling MMCs. Among these, PCD tools have the best wear and BUE resistant, and carbide tools show acceptable hole quality and wear [1,7]. It is also stated that WC drills can be used for small lot production especially at lower cutting speeds and higher feed rates [18] while PCD drills might be used for large lot production in terms of investment cost [2]. However, the high cost of the PCD tools limits the preferability of these tools. Researchers suggested that HSS and ceramic cutting tools are not suitable for drilling metal matrix composites due to excessive tool wear and poor surface quality. More than that, TiN coating on the HSS drills does not considerably increase the tool performance with respect to the uncoated ones [1,2,7,18].

Even though there has been some contradictory studies [1,10], many researchers reported that tool wear slightly increases with increasing cutting speed, but this effect is insignificant when drilling Al matrix composites [2,3,5,6,21]. Due to increasing cutting forces and torques at lower speeds, the effect of cutting speed on the tool wear become more important, especially at lower cutting speeds and less important at higher speeds [1].

Up to now, dimensional accuracy and profile of the drilled hole have been studied together with the tool wear [19,23−26]. It is argued that BUE formation increases when drilling with dry and conventional cooling, and this condition results in widening the tool cutting edge causing higher hole diameters [20]. On the other hand, if the corner wear of the cutting tool increases, the drill diameter can decrease depending on the produced hole number. For this reason, hole dimensional accuracy depends on the tool wear, drilled hole number and BUE formation. For example, in an earlier study, although hole size decreased depending on the tool wear between the first and the 20th hole, there was an increase in the hole diameters as the hole number increased more [19]. Another study on the investigation of the effect of cutting tool coating material on the drilled hole size and profile was performed under dry and coolant conditions with three types of cutting tools [23]. TiAlN/TiN coated drills showed better dimensional accuracy than the uncoated drills under the wet cutting conditions. However, under dry cutting conditions, dimension of the upper side of the produced hole was larger than that of the lower side due to the thermo-elastic deformation through the hole walls. Additionally, the hole diameter from the upper side through the bottom was less steady with dry and conventional cooling than with through-spindle cooling. Cooling with through-spindle cutting fluid produces

better hole quality than spray mist method [26]. According to another study on the effect of cutting parameters, tool tip angle and coating materials on the hole size, HSS drills having 5% cobalt showed better performance compared to TiN, TiNAlN coated and uncoated drills. On the other hand, the tool tip angle has a more important effect on the hole diameter than the other cutting parameters [25].

The aim of this study was to investigate the wear mechanisms as well as the hole diameter accuracy, and to introduce the Taguchi method in determining optimum drilling conditions on the tool's flank wear and hole dimensional accuracy when drilling Al 7xxx alloy (Al−5%Zn−3.5%Cu−2.5%Mg) reinforced with three different contents of B_4C particles. The drilling parameters were set by Taguchi's L_{27} orthogonal array. After the drilling experiments with HSS, TiAlN coated and solid carbide drills, tool wear phenomena were evaluated. Furthermore, the influence of the tool's corner and flank wear on the dimensional accuracy of the hole was analyzed. Grey relational analysis was applied to investigate how the cutting parameters affect the quality targets of the tool wear and hole dimensional accuracy. The analysis of variance (ANOVA) was conducted for the factors, and their contribution rates were determined. This work will be a good guide for selecting optimal machining parameters for the tool flank wear and diametral error of the drilled hole.

3 Experimental

3.1 Composite material production

Composite materials consisting of 10% B_4C, 15% B_4C and 25% B_4C were produced by PM method in prismatic dimensions of 50 mm×70 mm×12 mm. This method was similar to the fabrication route used by previous researchers [27]. The powder with average sizes of 8 μm for Zn, 15 μm for Cu and 30 μm for B_4C and Al were used for composite productions. For this purpose, metal powders of Al, B_4C, 3.5% Cu, 5% Zn and 2.5% Mg were weighed with Symmetry EC4000 electronic balance having 0.1 g accuracy and then uniformly mixed in a mixing bowl. The ball milling method, having 36 ZrO_2 balls, was used for mixing of the powders. After packing the mixture with Al foil, it was cold pressed into the mold under 25 MPa. Later, in order to fill the voids between metal and ceramic powders with Zn, the furnace temperature was kept at a constant temperature of 540 °C and composite specimens were fabricated by liquid phase sintering for 0.5 h at the temperature. Finally, the mold was kept inside the furnace until the furnace temperature reached 250 °C and then placed in the open air to complete the cooling. Hardness and tensile tests were also performed on the produced composites.

3.2 Experimental setup and drilling process

In this work, Taguchi method which is a useful tool for the design of performance characteristics was used [28]. L_{27} (3^{13}) orthogonal array was chosen since it has the ability to control the interactions among the factors [8, 29, 30]. For drilling experiments, the control factors and the levels of each parameter are given in Table 1.

Table 1 Drilling parameters and levels

Control parameters	Unit	Level		
		1	2	3
Content of B_4C (A)	%	10	15	25
Feed rate (B)	mm/r	0.1	0.2	0.3
Spindle speed (C)	r/min	1500	2000	2500
Drill material (D)		HSS	Carbide	TiAlN coated carbide

108 drilling experiments were carried out with CNC controlled vertical machining center under dry cutting conditions (Fig. 1(a)). Three different cutting tool materials, which were HSS, TiAlN coated and uncoated carbide, were used. The materials and geometrical properties of the cutting tools are listed in Table 2. Picture of the produced composite after the drilling test was depicted in Fig. 1(b).
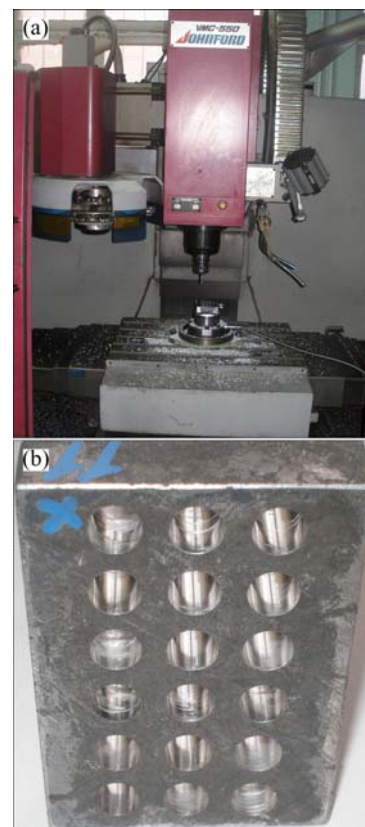

Fig. 1 Experimental set up and drilled workpiece: (a) Overview of CNC controlled vertical machining center; (b) MMC specimen after drilling test

Table 2 Cutting tool properties

Drill material	Drill diameter/mm	Drill type	Point angle/(°)	Helix angle/(°)	Clearance angle/(°)	Manufacturer	Hardness (HV)
HSS	8	Spiral	135	30	10	Format prof. quality	880
Uncoated carbide	8	Spiral	140	30	10	Kennametal	1500
TiAlN coated carbide	8	Spiral	140	30	10	Kennametal	2800

3.3 Measurement of tool wear and hole diameter

Wears of flank and corner were measured with a Mitutoyo–TM–20X optical microscope having 5 μm accuracy. For this aim, two special tool holders depending on the tool's tip angle, one for HSS tools at 67.5° and the other for carbide tools at 70°, were manufactured in order to keep the cutting tool edge parallel to the horizontal (Fig. 2). A similar method was used by AHAMED et al [10]. Additionally, in order to examine the wear mechanisms, drill bits were cut into 5 mm distance by using wire EDM machine, and scanning electron microscope (SEM) images of the cut drills were taken.
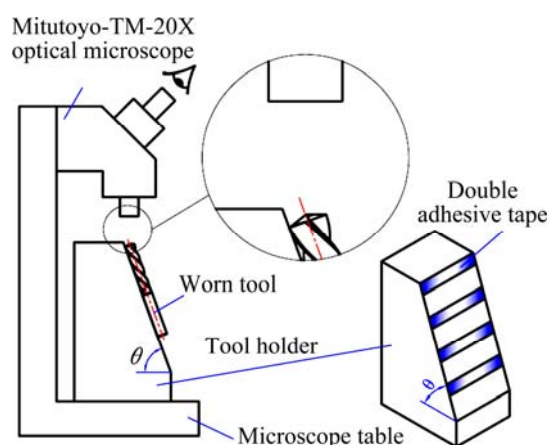

Fig. 2 Measuring method of flank wear, θ=67.5º for HSS tools, θ=70° for carbide tools

The measurement of the hole size is of significant importance for a variety of applications [31]. For evaluating the dimensional accuracy, hole diameters were measured with the ABERLINK-AXIOM II 965 CNC CMM machine having 0.1 μm accuracy. Two measurements were made at 5 mm distance from the hole entrance and hole-exits for each hole. Total error of the hole diameters was used.

4 Results and discussion

4.1 Microstructure and mechanical properties

SEM image of the fabricated composite specimen having 10% B_4C reinforcement was presented in Fig. 3 where black powders indicate B_4C and the others indicate the metal matrix content. A homogeneous distribution of the ceramic particles over the composite

alloy can be seen from this figure. The Zn, whose melting temperature is lower than that of other metals, transformed into liquid phase and filled the voids between metal and ceramic powders. Tensile and hardness test results of the produced composites are listed in Table 3. The hardness of the composites increased as the reinforcement rate increased due to the hard nature of the ceramic particles. Moreover, ultimate tensile strength (UTS) increased with an increase in the content of B_4C particles, and it was much higher than that for pure Al (90 MPa) and Al 7075 alloy (220 MPa) [32]. The results showed that UTS improved as increasing the particle mass fraction until the 15% B_4C which was an optimum fraction with regard to the strength. The reduction in UTS can be attributed to the size, sharp-edged and separation of the particles at some locations as well as poor bonding with the Al matrix [33].
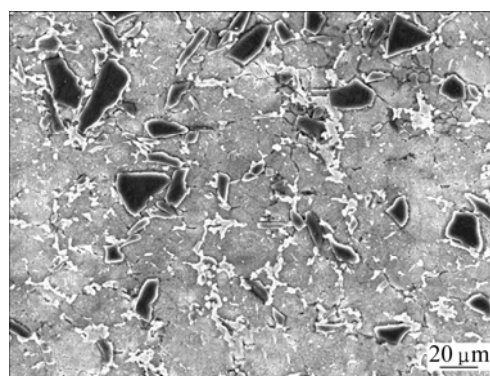

Fig. 3 SEM image of composite with 10% B_4C

Table 3 Tensile test and hardness results of produced composites

Mass fraction of B_4C particle/%	Yield strength/ MPa	Tensile strength/ MPa	Elongation/ %	Area reduction/ %	Hardness, HRB
10	491	527	22.2	1.113	61
15	532	599	6.87	2.110	79
25	328	408	4.8	3.870	87

4.2 Tool wear

Figure 4 illustrates typical wear types and BUE formation developed during the drilling process. Flank wear of the tool gets larger starting from the drill center toward the drill corner due to increasing peripheral speed

of the points on the drill bit [34]. For this reason, the highest tool wear occurs at the drill corner where the cutting speed and contact length are at maximum and where the cutting tool is subjected to both horizontal and vertical forces. According to the experimental results, the most important tool wear mechanism was abrasive wear, and no edge chipping was observed after drilling for one time each drill. B_4C particles, with hardness HV 4200, caused flank wear extending from chisel edge to the drill corner through the cutting edge. This flank wear growing from the cutting edge through the flank surface was caused by the abrasive effect of B_4C particles [4,7,10].

The tool wear is related to the time and nature of the tool-workpiece contact. Increase of the temperature,

contact time and abrasive effects of the ceramic particles specifies the tool wear. For example, since the contact time is relatively higher at the combination of lower cutting speeds and lower feed rates, the tool wear increases. This condition can be attributed to the fact that abrasive wear mechanism at the tool's flank face is dominant at lower cutting speeds. Although diffusion wear is effective at higher cutting speeds for nonferrous materials due to higher cutting temperatures, generally abrasive wear is more dominant when machining MMCs. Regarding the effect of the feed rate on the tool wear, it is known that tool wear decreases with increasing feed rates due to lower cutting time [1,10]. Figure 5 depicts the effects of the drilling parameters on the flank wear.
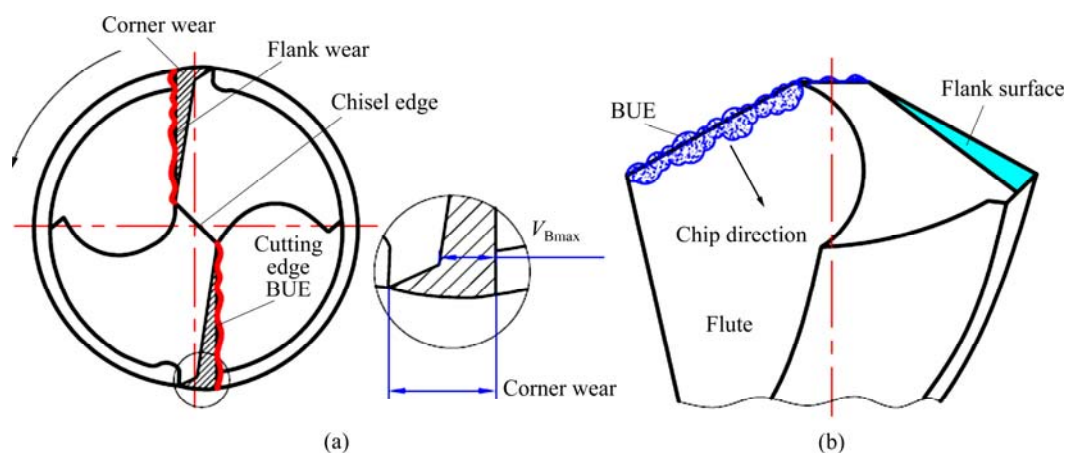

Fig. 4 Wear types of cutting tool: (a) Top view; (b) Front view
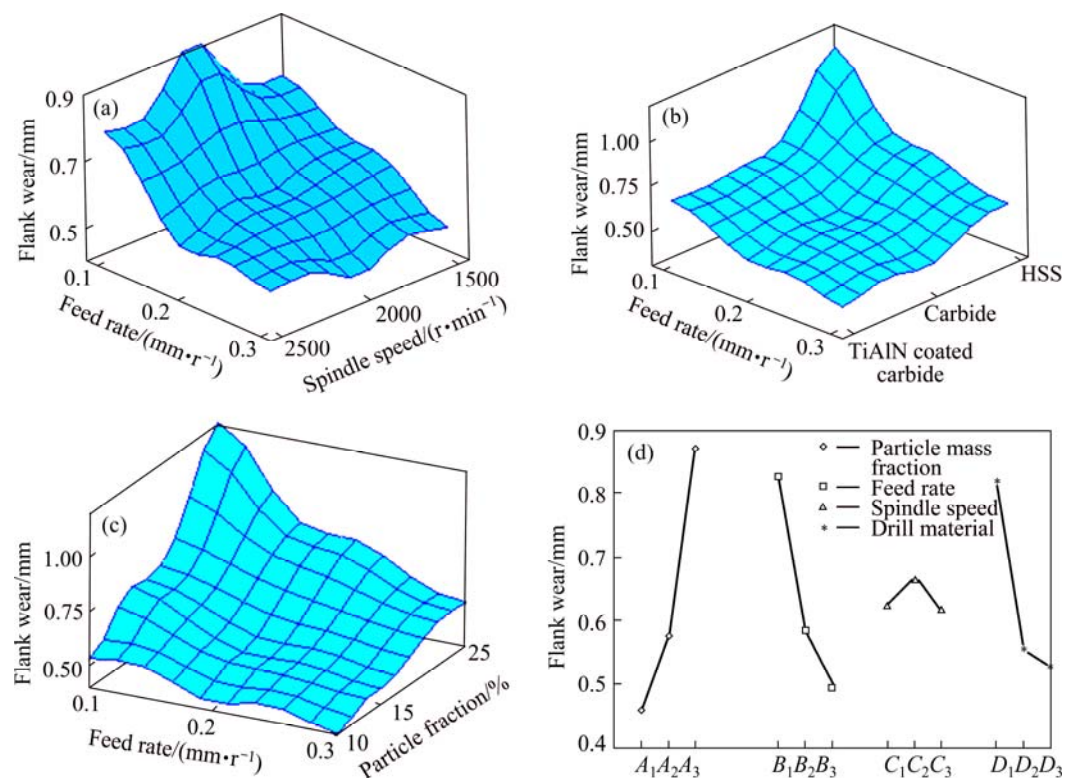

Fig. 5 Effects of process parameters on flank wear (VB) according to: (a) Feed rate and spindle speed; (b) Feed rate and cutting tool; (c) Feed rate and particle mass fraction; (d) Mean response graphs for flank wear

It can be deduced from Fig. 5(a) that the tool wear can improve if the feed rate is increased over the used range of feeds. Besides, the rate of increase in the flank wear for HSS tools was higher than that for carbide tools (Fig. 5(b)).

Figure 5(c) shows the flank wear variation with particle fraction and feed rate. From this figure, one can understand that flank wear increases with reinforcement content for all feed rates. The reason was that contact ratio between the B_4C particles and the cutting edge increased with increasing the content of the abrasive particles in the composite. Furthermore, there was more rubbing activity against the abrasive B_4C particulates. This idea was supported by previous studies stating that abrasive forces and thus wear rate increased when the density of the hard particle increased [4,35].

Figure 5(d) presents the response graphs regarding the effects of the factors on the tool wear. From the point of view of the cutting speed, the results of Fig. 5(d) shows that increasing the spindle speed do not significantly influence the tool wear. Moreover, variations in the tool wear as a function of spindle speed are weak compared to that of particle fraction or feed rate (Fig. 6). The reason was that the tool wear mechanisms on the machining of ferrous and nonferrous materials were different. For example, flank and crater wear grow with increasing the cutting speed during the drilling of ferrous materials and certain high strength alloys due to higher interface temperature between the cutting tool and workpiece [2]. However, an increase in the cutting speed has a less influence on cutting temperature at the interface during the drilling of nonferrous materials. Accordingly, cutting speed does not significantly affect the cutting of Al since the melting temperature of the Al alloys (550−660 °C) is close to the softening temperature of the HSS tools (540−600 °C) and is much smaller than that of carbide tools (870−1100 °C) [36]. Furthermore, the machining forces and temperatures are usually small due to good heat conductivity of the aluminum. For this reason, majority of the generated heat during the cutting is dissipated outside the drilled hole [35]. As a result, although some of the past studies claimed that flank wear increases somewhat with increasing cutting speed [9,10], most of them asserted cutting speed play a minor role on the tool's flank wear when machining Al alloys [2,3,5,6]. But in many of the cases, the tool damage is caused by adhesion of the machined material on the tool surface.

In addition to the abrasive wear because of hard ceramic particles, diffusion wear was also expected owing to ductile Al when machining Al matrix composites. The material transfer from the cutting tool through the chip causes the formation of adhesion layer, BUE or crater on the rake face. The BUE has important
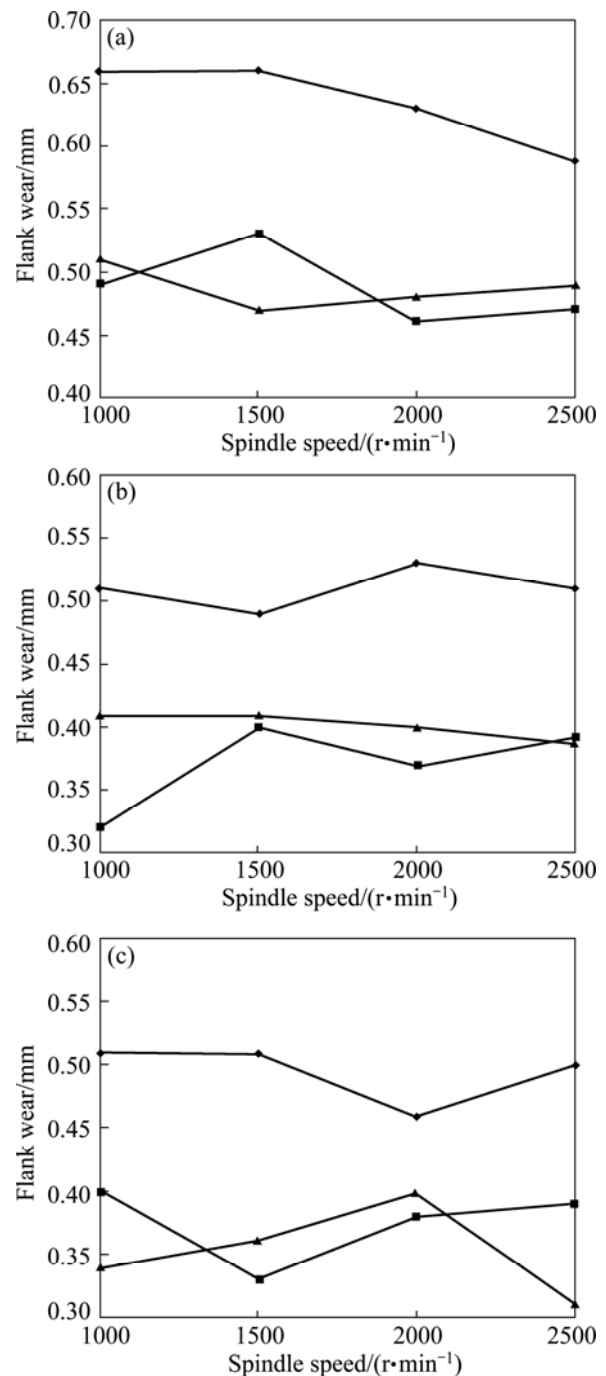

Fig. 6 Flank wear according to cutting speed when drilling 10% B_4C composites: (a) f=0.1 mm/r; (b) f=0.2 mm/r; (c) f=0.3 mm/r

effects on the machining forces, temperatures, friction coefficient, size accuracy of the machined parts, surface finish, chip size, tool life, and so on. In practice, BUE, which is an irregular and unstable structure formed mainly on the rake face during machining ductile alloys, is greatly influenced by cutting conditions, workpiece and tool material. Generally, BUE is formed under lower cutting speeds and higher feed rates [37,38]. However there is a conflicting study arguing that adherent layer continuously increases at higher cutting speeds, leading

to accumulation of chip material on the cutting edge [39]. Additionally, the heat treated materials or those having more hardness were subjected to less BUE formation. The SEM microstructure of the worn flank surface of HSS tool under 0.3 mm/r feed rate, 1000 r/min spindle speed, 10% B_4C particle fraction is shown in Fig. 7. From the figure, one can observe that BUE was formed mostly at the tool's rake face and chisel edge since the cutting speed close to the chisel edge was very low. Moreover, micro grooves, indicating that the major wear mechanism was abrasive wear, were also produced parallel to the cutting direction due to abrasive B_4C particles, as seen in Fig. 7(b). In this work, BUE formation increased with lower particle fraction at higher feed rates. Moreover, with uncoated and coated carbide tools, considerably less BUE formation was observed than HSS tools, as seen in Figs. 8(a) and (b). The reason was that coated tools prevented the diffusion and adhering activity by making a thermal barrier. In addition, lesser micro grooves caused by abrasive B_4C particles were detected with coated and uncoated carbide tools compared with HSS tools.

In addition to all of these, cutting tools were tested for the purpose of determining the variation of tool wear when drilling two holes successively with 1000 and 1500 r/min spindle speeds, and 0.1, 0.2 and 0.3 mm/rev feed rates. The composite specimens having 25% B_4C could not have been drilled continuously two times with HSS tools. Figure 9 represents the results of the flank and corner wear values for single and successive two drillings of 15% B_4C composite at 1500 r/min spindle speed. Furthermore, after two successive drillings, the rate of increase in the tool wear for HSS tools was found to be more than that of the carbide tools compared to single drilling especially at lower feed rates. Decreasing of tool wear with increasing feed rate at both single hole and successive two-holes drillings can be clearly seen from these figures. Additionally, Fig. 9 indicates that cutting tool hardness is very important for abrasive wear, and HSS drills are not suitable for drilling of B_4C reinforced MMCs. More than that, BUE formation increased after all of the successive two hole drilling operations for all cutting tools. No edge chipping and breakage were observed after the two successive drilling, similar to the single drilling.

4.3 Hole dimensional accuracy

The produced hole diameter depends on the drill's corner wear, BUE formation and dynamic behavior of the machine tool and cutting tool. If the abrasive corner
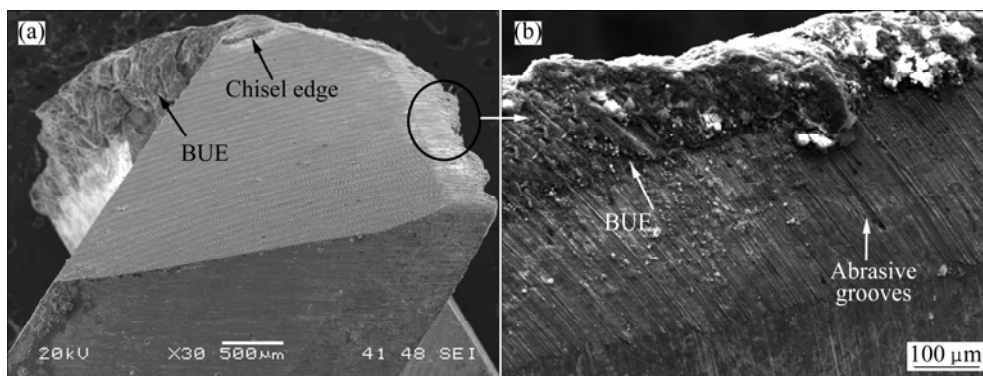

Fig. 7 SEM images of HSS drill at n=1000 r/min, f=0.3 mm/r with 10% B_4C: (a) BUE formation at rake face and flank face; (b) Higher magnification of flank face
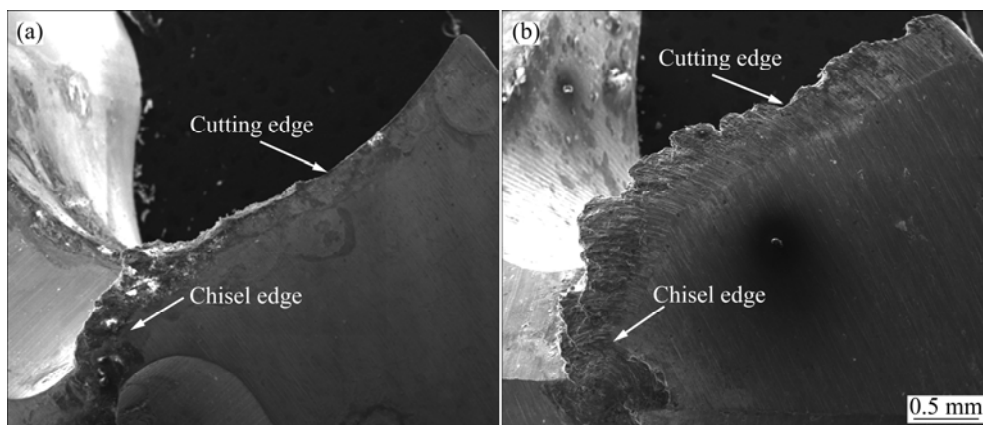

Fig. 8 SEM images of drills at n=2000 r/min, f=0.2 mm/r and 10% B_4C: (a) Solid carbide tool; (b) HSS tool

wear exhibit more dominant character than BUE formation, drill diameter might decrease due to decreasing drill diameter. Otherwise drill diameter might increase because of severe BUE formation especially when drilling many number of holes [19,20]. In this work, generally, produced hole diameters decreased with the tool wear for all drill bits due to corner wear. For 108 drilling experiments, lower and upper limit values of the hole diameters were found to be 7.959 and 8.14 mm, respectively. In terms of the hole dimensional accuracy, the best results were obtained with coated carbide drill

since coating material limited the diffusion action making a thermal barrier.

Figure 10 shows the effects of drilling parameters on the size variation of the drilled hole. This figure reveals that there is significant variation of the hole size with regard to the cutting speed and drill material. At higher spindle speeds, the chatter vibrations as well as dynamic behavior of the cutting tool changes, increasing the variation of the diametral error. Regarding the drill bit material, lower size errors were obtained with carbide tools than HSS tools. TiAlN coated carbide tools showed
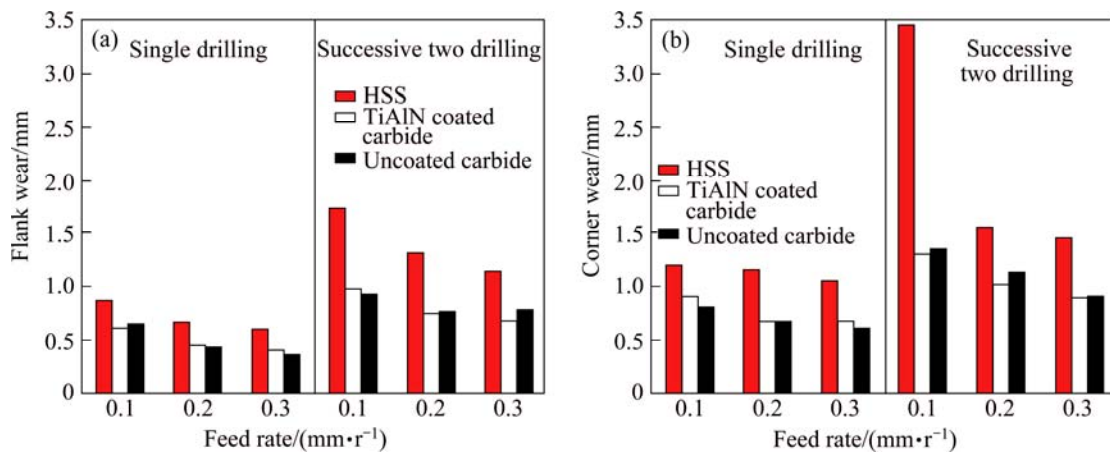

Fig. 9 Tool wear for single and successive two drilling of 15% B_4C composite at 1500 r/min: (a) Flank wear; (b) Corner wear
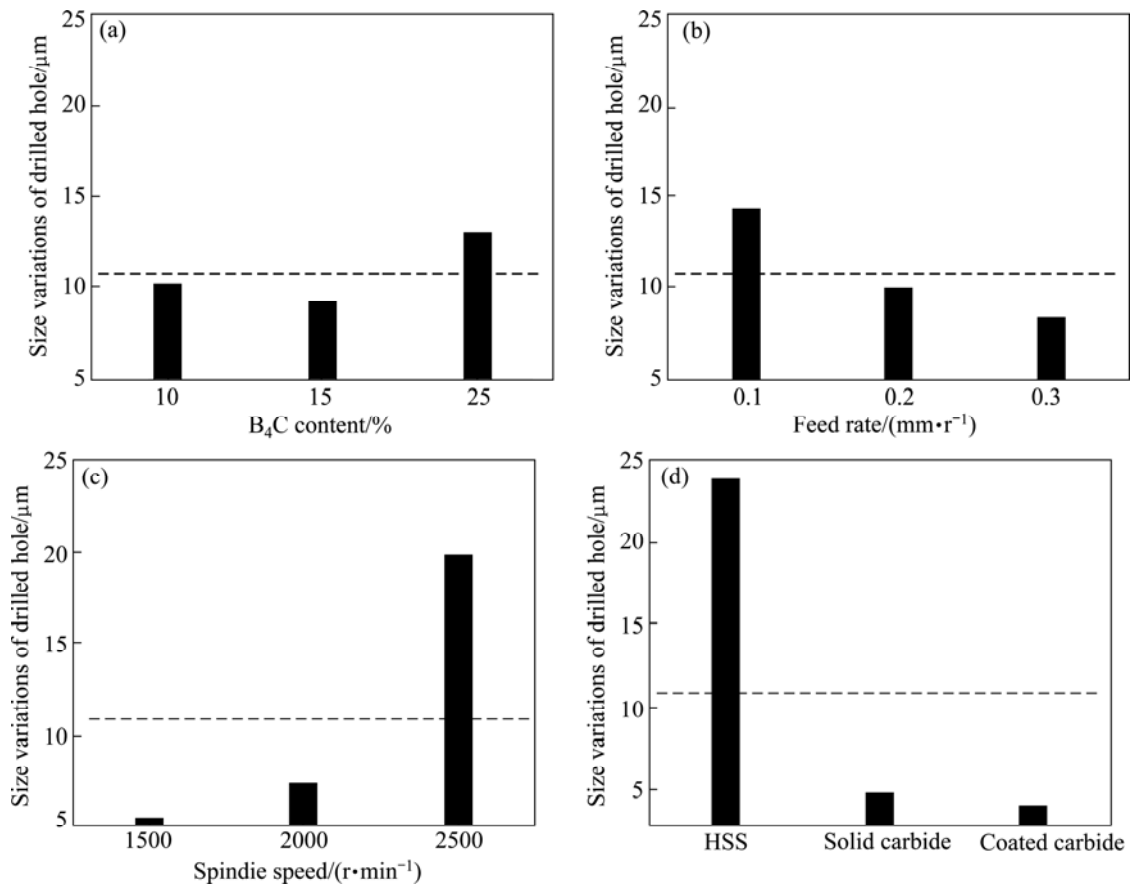

Fig. 10 Effects of factors on mean size variation of drilled hole

the best performance with regard to the hole size. Furthermore, the diametral error was smaller when drilling composites having less B₄C content. This condition can be explained by spring back phenomena that richer Al matrix material expanded and then contracted because of the temperature fluctuations [25,40]. Minimum size error was obtained with 15% B₄C content, but at higher reinforcement fractions, tool's corner wear increased, leading to more size variations. As a conclusion, the optimal machining conditions for the hole quality were obtained as 15% B₄C content, 1500 r/min spindle speed and 0.3 mm/r feed rate with TiAlN coated carbide drill.

4.4 Multi response optimization with grey relational analysis (GRA)

In this work, drilling parameters were optimized with GRA, a valuable methodology for the design of qualitative and discrete parameters. With this method, the experimental data were analyzed to obtain the influence of design parameters and to measure the correlation between the multi responses [41,42]. For this purpose, after the normalization of the experimental results, a gray relational grade was determined to assess the multiple responses. Importance order of the influence of design parameters on the multi responses (tool wear and hole size variation) was determined. In order to optimize the process parameters, the following steps are shown as follows:

1) The experimental results are normalized (data pre-processing).

2) The grey relational coefficient and grey relational grade are computed.

3) The experimental results are analyzed.

4) The optimal levels of the process parameters are selected.

5) The optimal parameters through the confirmation experiments are verified.

4.4.1 Normalization of responses

The results of the experiments for the total diametral error (d_e) and tool's flank wear (V_B) conducted by using $L_{27}(3^{13})$ orthogonal array are given in Table 4. For calculating the grey grade, tool wear and diametral error values were normalized in the range between zero and one [43]. This process is called the data pre-processing and is required due to being different range and unit of each data. Data pre-processing transfers the original sequence to a comparable one. There are several methods of data pre-processing such as "smaller better", "larger better" and "nominal better" depending on the characteristics of a data sequence for the grey relational analysis. In this wrok, calculation method of

"smaller better" was used since minimization of the tool wear and diametral error was intended. For calculating the normalized value of jth response of kth experiment $Z_j(k)$, the following expression can be used:

$$Z_j(k) = \frac{\max_j[Y_j(k)] - Y_j(k)}{\max_j[Y_j(k)] - \min_j[Y_j(k)]} \quad (1)$$

where $Y_j(k)$ is the original value to be normalized; $\max_j[Y_j(k)]$ is the largest value of $Y_j(k)$, $\min[Y_j(k)]$ is the smallest value of $Y_j(k)$.

For example, the normalized value for $j=1−2$, $k=1−27$ can be computed as follows:

$$Y_1(1) = (110−18)/(110−1) = 0.844 \quad (2)$$

$$Y_2(1) = (1.78−0.66)/(1.78−0.36) = 0.789 \quad (3)$$

The normalized values for the tool wear and diametral error are presented in Table 4.

4.4.2 Computing grey relational coefficient

Regarding the grey relational analysis, the degree of the relevancy between two systems is defined as the grey relational grade. Grey relational coefficient $\varepsilon(k)$ was calculated to express the relationship between the ideal and actual normalized experimental results. The grey relational coefficient can be expressed as follows [41,42, 44,45]:

$$\varepsilon_j(k) = (\min_j \min_k |Z_j(k) - Z_0(j)| +$$

$$\xi \max_j \max_k |Z_j(k) - Z_0(j)|)/(|Z_j(k) - Z_0(j)| +$$

$$\xi \max_j \max_k |Z_j(k) - Z_0(j)|) \quad (4)$$

where $Z_0(j)$ is the ideal sequence which is the value of 1, $\varepsilon_j(k)$ is the grey relational coefficient of jth performance characteristic of kth experiment.

Distinguishing coefficient ξ is defined in the range $0 \leq \xi \leq 1$. It is generally taken as 0.5. If this coefficient was small, distinguishing capability would be higher (the value may be adjusted based on the practical needs of the system).

4.4.3 Grey relational grade

Grey relational grade (average value of the grey relational coefficients) is the measure of geometrical similarity between Z_0 and Z_j in a grey system and it can take a value between 0−1. A higher grey relational grade indicates a strong relational degree between the comparative and the ideal sequence. Grey relational grade γ_k for the kth experiment can be determined from the following equation:

$$\gamma_k = \frac{1}{n}\sum_{j=1}^{n}\varepsilon_j(k) \quad (5)$$

where n is the number of responses.

For example, the grey relational grade for factor diametral error (d_e) at level 1 can be calculated by

Table 4 Taguchi experimental design, normalized values and grey grades for diametral error and tool wear

Exp. No	Coded factor				Experimental result (Y_j)		Normalization (Z_j)		Grey relation coefficient (ε_i)		Grey grade (γ)	Optimum order
	A	B	C	D	d_e/μm	V_B/mm	d_e	V_B	d_e	V_B		
1	1	1	1	1	18	0.66	0.844	0.789	0.762	0.703	0.733	19
2	1	1	2	2	13	0.46	0.890	0.930	0.820	0.877	0.848	13
3	1	1	3	3	7	0.49	0.945	0.908	0.901	0.845	0.873	11
4	1	2	1	2	1	0.4	1.000	0.972	1.000	0.947	0.973	1
5	1	2	2	3	6	0.4	0.954	0.972	0.916	0.947	0.931	5
6	1	2	3	1	91	0.51	0.174	0.894	0.377	0.826	0.601	22
7	1	3	1	3	6	0.36	0.954	1.000	0.916	1.000	0.958	2
8	1	3	2	1	25	0.46	0.780	0.930	0.694	0.877	0.785	17
9	1	3	3	2	11	0.39	0.908	0.979	0.845	0.959	0.902	7
10	2	1	1	2	4	0.65	0.972	0.796	0.948	0.710	0.829	15
11	2	1	2	3	3	0.61	0.982	0.824	0.965	0.740	0.852	12
12	2	1	3	1	110	0.93	0.000	0.599	0.333	0.555	0.444	27
13	2	2	1	3	1	0.45	1.000	0.937	1.000	0.888	0.944	3
14	2	2	2	1	22	0.63	0.807	0.810	0.722	0.724	0.723	20
15	2	2	3	2	2	0.48	0.991	0.915	0.982	0.855	0.919	6
16	2	3	1	1	5	0.6	0.963	0.831	0.932	0.747	0.839	14
17	2	3	2	2	5	0.41	0.963	0.965	0.932	0.934	0.933	4
18	2	3	3	3	10	0.42	0.917	0.958	0.858	0.922	0.890	9
19	3	1	1	3	23	0.91	0.798	0.613	0.712	0.563	0.638	21
20	3	1	2	1	41	1.78	0.633	0.000	0.577	0.333	0.455	26
21	3	1	3	2	32	0.95	0.716	0.585	0.637	0.546	0.592	23
22	3	2	1	1	32	1.06	0.716	0.507	0.637	0.504	0.570	24
23	3	2	2	2	8	0.72	0.936	0.746	0.886	0.664	0.775	18
24	3	2	3	3	8	0.615	0.936	0.820	0.886	0.736	0.811	16
25	3	3	1	2	2	0.54	0.991	0.873	0.982	0.798	0.890	10
26	3	3	2	3	2	0.515	0.991	0.891	0.982	0.821	0.901	8
27	3	3	3	1	79	0.76	0.284	0.718	0.411	0.640	0.525	25

averaging the grey relational coefficients as follows:

$$\gamma_{A1} = \frac{1}{2}(0.762 + 0.703) = 0.733 \qquad (6)$$

The results of calculated grey relational coefficients $\varepsilon_j(k)$ ($j=1, \cdots, 2$) and grey relational grade γ_k ($k=1, \cdots, 27$) using Eqs. (4) and (5), respectively, for different cutting conditions are given in Table 4. The calculated grey relational grades for each experiment were put in order from maximum (optimum) to minimum and then they are presented in the rightmost of the Table 4. The optimal value, which was the maximum of the grey relational grade, was found to be 4th experiment (Table 4).

In the next step, the main effects of each factor were calculated from the value of grey relational grade. The

maximum grey relational grades of each factor were calculated (Table 5) and the effects of the factors are plotted in Fig. 11. By maximizing the grade values (Table 5 and Fig. 11), minimum of the tool wear and diametral error can be obtained at the $A_1B_3C_1D_3$ optimal machining conditions.

Table 5 Main effects of factors on grey grade

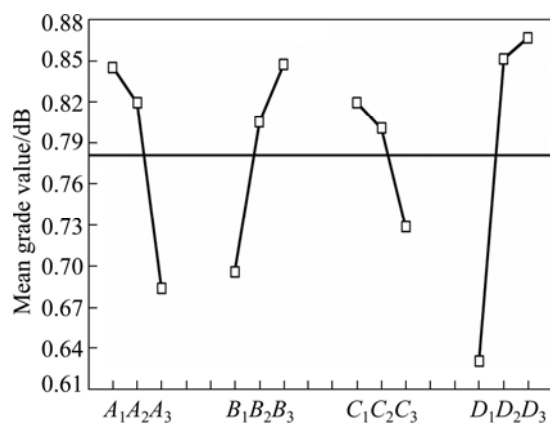| Factor	Unit	Level		
		1	2	3
Particle fraction (A)	%	0.845*	0.819	0.684
Feed rate (B)	mm/r	0.696	0.805	0.847*
Spindle speed (C)	r/min	0.819*	0.800	0.729
Drill material (D)	HV	0.631	0.851	0.867*

*Levels for optimum grey relational grade.

Fig. 11 Effect of each factor with regard to multiple performance on grey grade

4.5 Analysis of variance (ANOVA)

After analyzing the effect of machining parameters on the grey relational grade, the relative importance among the drilling parameters for multiple performance characteristics is analyzed in order to find more definitely the optimal combinations of the drilling parameter levels. For this purpose, analysis of variance (ANOVA) is applied to determine which parameter significantly influences the performance characteristic. According to the ANOVA results presented in Table 6, the most efficient factor on the grey grade was found to be drill material as 47.4%, followed by the particle fraction (20.33%) and feed rate (16.62%). However, the effect of spindle speed (6.25%) was found to be the lowest of all other factors.

Table 6 ANOVA results for grey grade

Factor	DF	SS	V	F-test	PD
Particle fraction (A)	2	0.1343	0.0672	14.298	20.33
Feed rate (B)	2	0.1098	0.0549	11.681	16.62
Spindle speed (C)	2	0.0413	0.0206	4.383	6.25
Drill material (D)	2	0.3131	0.1566	33.319	47.4
$A \cdot B$	4	0.0250	0.0063	1.340	3.79
$A \cdot C$	4	0.0036	0.0009	0.192	0.54
$B \cdot C$	4	0.0051	0.0013	0.277	0.77
Error	6	0.0284	0.0047		4.3
Total	26	0.6606			100

DF: Degree of freedom; SS: Sum of squares; V: Variance; PD: Percentage distribution; F-table$_{(0.05;2;6)}$=5.14; F-table$_{(0.05;4;6)}$=4.53

4.6 Verification process through confirmation experiments

In the final step, prediction and verification of the performance characteristics regarding the selected initial parameter setting were carried out. Grey relational grade at the optimum conditions $\gamma_{\text{predicted}}$ was predicted by using the following model:

$$\gamma_{\text{predicted}} = \gamma_{\text{m}} + \sum_{i=1}^{N}(\gamma_0 - \gamma_{\text{m}}) \tag{7}$$

where γ_{m} is the total mean of the grey relational grade, γ_0 is the mean grey relational grade at optimal level, and N is the number of main design parameters that significantly affect the multiple performance characteristics [28].

The predicted grey grade by Eq. (7) was found to be as 1.02 for the machining conditions of $A_1B_1C_3D_3$. The difference between the experimental result (0.958) and the predicted result (1.02) was 6.5%. This result is within the confidence interval of the predicted optimal condition. In addition, Figure 12 shows the comparison between the predicted and the experimental grey grades at different cutting conditions. These results show that the predicted results are compatible with the confirmation experiments. Thus, the grey relational analysis is a very powerful method for estimating the grey relational grade in the drilling of Al/B$_4$C reinforced MMCs.
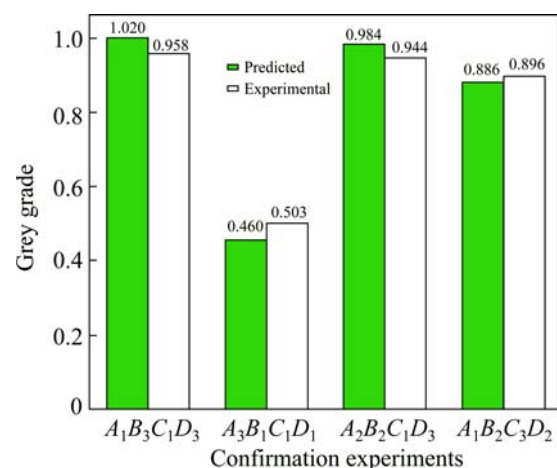

Fig. 12 Results of confirmation experiments

5 Conclusions

Drilling experiments of MMCs were carried out to study the effects of machining parameters such as particle mass fraction, drill material, spindle speed and feed rate on the tool wear and dimensional accuracy of the drilled hole. Machining parameters were optimized based on the grey relational analysis. According to the experimental results, mostly abrasive wear and BUE were observed in the cutting tools, and the tool wear increased with particle mass fraction and decreased with feed rate. However, cutting speed had less effect on the tool wear than the other machining parameters over the used range of speeds. Additionally, higher BUE formation was observed with HSS tools than TiAlN coated carbide tools but uncoated tools were subjected to

greater BUE than the coated drills. BUE formation increased as feed rates increased and particle mass fraction decreased. With regard to the dimensional accuracy, it was seen that the produced hole sizes were negatively affected by the tool wear, and the best results were obtained with coated carbide drills. Generally, produced hole diameters decreased with the tool wear for majority of the tools. The influence of the particle fraction on the hole size variation was not high. From the grey relational analysis, the largest grey relational grade was found for the B_4C particle content of 10%, feed rate of 0.3 mm/r, spindle speed of 1500 r/min and drill material of TiAlN coated carbide. These were the recommended levels of the drilling parameters when the minimization of the tool wear and diametral error are simultaneously considered.

Acknowledgments

References

[1]   MONAGHAN J, O'REILLY P. The drilling of an Al/SiC metal-matrix composite [J]. Journal of Materials Processing Technology, 1992, 33: 469−480.

[2]   COELHO R T, YAMADA S, ASPINWALL D K, WISE M L H. The application of polycrystalline diamond (PCD) tool materials when drilling and reaming aluminium based alloys including MMC [J]. International Journal of Machine Tools and Manufacture, 1995, 35: 761−774.

[3]   MORIN E, MASOUNAVE J, LAUFER E E. Effect of drill wear on cutting forces in the drilling of metal-matrix composites [J]. Wear, 1995, 184: 11−16.

[4]   SONGMENE V, BALAZINSKI M. Machinability of graphitic metal matrix composites as a function of reinforcing particles [J]. CIRP Annals - Manufacturing Technology, 1999, 48: 77−80.

[5]   DAVIM J P, CONCEIÇÃO ANTÓNIO C A. Optimal drilling of particulate metal matrix composites based on experimental and numerical procedures [J]. International Journal of Machine Tools and Manufacture, 2001, 41: 21−31.

[6]   DAVIM J P, MONTEIRO BAPTISTA A. Cutting force, tool wear and surface finish in drilling metal matrix composites [J]. Proceedings of the Institution of Mechanical Engineers, Part E: Journal of Process Mechanical Engineering, 2001, 215: 177−183.

[7]   RAMULU M, RAO P N, KAO H. Drilling of $(Al_2O_3)p/6061$ metal matrix composites [J]. Journal of Materials Processing Technology, 2002, 124: 244−254.

[8]   DAVIM J P. Study of drilling metal-matrix composites based on the Taguchi techniques [J]. Journal of Materials Processing Technology, 2003, 132: 250−254.

[9]   KARAKAŞ M S, ACIR A, ÜBEYLI M, ÖGEL B. Effect of cutting speed on tool performance in milling of B_4C_p reinforced aluminum

[10] AHAMED A R, ASOKAN P, ARAVINDAN S, PRAKASH M K. Drilling of hybrid $Al−5\%SiC_p−5\%B4Cp$ metal matrix composites [J]. International Journal of Advanced Manufacturing Technology, 2010, 49: 871−877.

[11] SEEMAN M, GANESAN G, KARTHIKEYAN R, VELAYUDHAM A. Study on tool wear and surface roughness in machining of particulate aluminum metal matrix composite-response surface methodology approach [J]. International Journal of Advanced Manufacturing Technology, 2010, 48: 613−624.

[12] RAJMOHAN K P T, PAULO DAVIM J. Analysis of surface integrity in drilling metal matrix and hybrid metal matrix composites [J]. J Mater Sci Technol, 2012, 23: 761−768.

[13] CANDAN S, BILGIC E. Corrosion behavior of $Al−60$ vol.% SiC_p composites in NaCl solution [J]. Materials Letters, 2004, 58: 2787−2790.

[14] BOŽIĆ D, STAŠIĆ J, RAJKOVIĆ V. Microstructures and mechanical properties of $ZA27-Al_2O_3$ composites obtained by powder metallurgy process [J]. Science of Sintering, 2011, 43: 63−70.

[15] ANANDAKRISHNAN V, MAHAMANI A. Investigations of flank wear, cutting force, and surface roughness in the machining of $Al-6061-TiB_2$ in situ metal matrix composites produced by flux-assisted synthesis [J]. International Journal of Advanced Manufacturing Technology, 2011, 55: 65−73.

[16] RAHIMIAN M, PARVIN N, EHSANI N. The effect of production parameters on microstructure and wear resistance of powder metallurgy $Al-Al_2O_3$ composite [J]. Materials and Design, 2011, 32: 1031−1038.

[17] CHOUDHURY S K, RAJU G. Investigation into crater wear in drilling [J]. International Journal of Machine Tools and Manufacture, 2000, 40: 887−898.

[18] KANNAN S, KISHAWY H A, BALAZINSKI M. Flank wear progression during machining metal matrix composites [J]. Journal of Manufacturing Science and Engineering, Transactions of the ASME, 2006, 128: 787−791.

[19] BARNES S, PASHBY I R, HASHIM A B. Effect of heat treatment on the drilling performance of aluminum/SiC MMC [J]. Applied Composite Materials, 1999, 6: 121−138.

[20] BARNES S, PASHBY I R. Through-tool coolant drilling of aluminum/SiC metal matrix composite [J]. Journal of Engineering Materials and Technology, Transactions of the ASME, 2000, 122: 384−388.

[21] PAULO DAVIM J, MONTEIRO BAPTISTA A. Relationship between cutting force and PCD cutting tool wear in machining silicon carbide reinforced aluminum [J]. Journal of Materials Processing Technology, 2000, 103: 417−423.

[22] LIST G, NOUARI M, GÉHIN D, GOMEZ S, MANAUD J P, LE PETITCORPS Y, et al. Wear behaviour of cemented carbide tools in dry machining of aluminium alloy [J]. Wear, 2005, 259: 1177−1189.

[23] KALIDAS S, DEVOR R E, KAPOOR S G. Experimental investigation of the effect of drill coatings on hole quality under dry and wet drilling conditions [J]. Surface and Coatings Technology, 2001, 148: 117−128.

[24] PIRTINI M, LAZOGLU I. Forces and hole quality in drilling [J]. International Journal of Machine Tools and Manufacture, 2005, 45: 1271−1281.

[25] KURT M, KAYNAK Y, BAGCI E. Evaluation of drilled hole quality in Al 2024 alloy [J]. International Journal of Advanced Manufacturing Technology, 2008, 37: 1051−1060.

[26] SHYHA I S, SOO S L, ASPINWALL D K, BRADLEY S, PERRY R, HARDEN P, et al. Hole quality assessment following drilling of metallic-composite stacks [J]. International Journal of Machine Tools

and Manufacture, 2011, 51: 569−578.

[27] YILBAS B S, KHAN S, RAZA K, KELES O, UBEYLI M, DEMIR T, et al. Laser cutting of 7050 Al alloy reinforced with Al_2O_3 and B_4C composites [J]. International Journal of Advanced Manufacturing Technology, 2010, 50: 185−193.

[28] RAJMOHAN T, PALANIKUMAR K. Optimization of machining parameters for multi-performance characteristics in drilling hybrid metal matrix composites [J]. Journal of Composite Materials, 2012, 46: 869−878.

[29] TSAO C C. Taguchi analysis of drilling quality associated with core drill in drilling of composite material [J]. International Journal of Advanced Manufacturing Technology, 2007, 32: 877−884.

[30] TSAO C C, HOCHENG H. Evaluation of thrust force and surface roughness in drilling composite material using Taguchi analysis and neural network [J]. Journal of Materials Processing Technology, 2008, 203: 342−348.

[31] KURT M, BAGCI E, KAYNAK Y. Application of Taguchi methods in the optimization of cutting parameters for surface finish and hole diameter accuracy in dry drilling processes [J]. International Journal of Advanced Manufacturing Technology, 2009, 40: 458−469.

[32] VEERESH KUMAR G B, RAO C S P, SELVARAJ N. Studies on mechanical and dry sliding wear of Al6061-SiC composites [J]. Composites Part B: Engineering, 2012, 43: 1185−1191.

[33] MANNA A, BAINS H S, MAHAPATRA P B. Experimental study on fabrication of Al-Al2O3/Grp metal matrix composites [J]. Journal of Composite Materials, 2011, 45: 2003−2010.

[34] LI R, SHIH A J. Tool temperature in titanium drilling [J]. Journal of Manufacturing Science and Engineering, Transactions of the ASME, 2007, 129: 740−749.

[35] ALRASHDAN A, MAYYAS A T, HASSAN A M, HAYAJNEH M T. Drilling of Al−Mg−Cu alloys and Al−Mg−Cu/SiC composites [J]. Journal of Composite Materials, 2011, 45: 2091−2101.

[36] HAMADE R F, ISMAIL F. A case for aggressive drilling of aluminum [J]. Journal of Materials Processing Technology, 2005, 166: 86−97.

[37] FANG N, PAI P S, EDWARDS N. Prediction of built-up edge formation in machining with round edge and sharp tools using a neural network approach [J]. International Journal of Computer Integrated Manufacturing, 2010, 23: 1002−1014.

[38] AKHAVAN FARID A, SHARIF S, IDRIS M H. Chip morphology study in high speed drilling of Al−Si alloy [J]. International Journal of Advanced Manufacturing Technology, 2011, 57: 555−564.

[39] NOUARI M, LIST G, GIROT F, GÉHIN D. Effect of machining parameters and coating on wear mechanisms in dry drilling of aluminium alloys [J]. International Journal of Machine Tools and Manufacture, 2005, 45: 1436−1442.

[40] HAYAJNEH M T. Hole quality in deep hole drilling [J]. Materials and Manufacturing Processes, 2001, 16: 147−164.

[41] HAQ A N, MARIMUTHU P, JEYAPAUL R. Multi response optimization of machining parameters of drilling Al/SiC metal matrix composite using grey relational analysis in the Taguchi method [J]. International Journal of Advanced Manufacturing Technology, 2008, 37: 250−255.

[42] PALANIKUMAR K. Experimental investigation and optimisation in drilling of GFRP composites [J]. Measurement: Journal of the International Measurement Confederation, 2011, 44: 2138−2148.

[43] RAJMOHAN T, PALANIKUMAR K, KATHIRVEL M. Optimization of machining parameters in drilling hybrid aluminium metal matrix composites [J]. Transactions of Nonferrous Metals Society of China: English Edition, 2012, 22: 1286−1297.

[44] TOSUN N. Determination of optimum parameters for multi-performance characteristics in drilling by using grey relational analysis [J]. International Journal of Advanced Manufacturing Technology, 2006, 28: 450−455.

[45] PALANIKUMAR K, LATHA B, SENTHILKUMAR V S, DAVIM J P. Analysis on drilling of glass fiber-reinforced polymer (GFRP) composites using grey relational analysis [J]. Materials and Manufacturing Processes, 2012, 27: 297−305.

钻削 B_4C 颗粒增强铝合金工艺参数对刀具磨损和孔尺寸精度影响的分析和优化

A. TASKESEN[1], K. KUTUKDE[2]

1. Manufacturing Engineering, Gazi University, 06500 Teknikokullar, Ankara, Turkey;
2. Institute of Science and Technology, Gazi University, 06500 Teknikokullar, Ankara, Turkey

摘　要：基于刀具磨损和钻孔尺寸误差等多个性能指标，对 B_4C 颗粒增强铝合金切削加工参数进行评估和优化。通过 Taguchi 的 L27，3 水平 4 因子正交阵列进行实验设计。研究结果表明：磨粒磨损和积屑瘤一般在刀具磨损时形成，同时，边角磨损也具有重大意义。影响切削刀具的侧面磨损主要决定因素是合金中的颗粒质量分数，其次分别是进给速率、钻头的硬度和主轴转速。在所有使用的刀具中，有 TiAlN 涂层的硬质合金钻头在刀具磨损以及孔尺寸方面具有最佳性能。灰关系分析表明：钻头材料的影响比进给速度和主轴转速的影响更大。在最佳的钻探参数下可以得到最小的刀具磨损和孔直径误差。

关键词：粉末冶金；B_4C；钻削；刀具磨损；孔尺寸精度；优化

(Edited by Chao WANG)